Chemical Analysis by Neutron Spectroscopy[1]

T. I. Taylor, Robert H. Anderson, and W. W. Havens, Jr.
Chemistry and Physics Departments, Columbia University, New York

DURING RECENT YEARS the neutron has served as a very useful tool for the study of certain nuclear and atomic properties of matter (*1*). Neutrons are now finding a number of important applications to the determination of the composition of materials (*2*). A review of the properties and interactions of neutrons (Table 1) shows that chemical analysis by neutron interactions is possible by several different methods.

TABLE 1

SUMMARY OF PROPERTIES AND INTERACTIONS OF NEUTRONS

General	Mass, 1.00893; charge, 0; spin, ± ½; half-life, 10–20 min; statistics, Fermi-Dirac.
Production	See Table 2.
Wave properties	$\lambda = \frac{h}{mv} = \frac{h}{\sqrt{2ME}}$ $\lambda(A) = \frac{3.96 \times 10^3}{v} = \frac{0.286}{\sqrt{E(ev)}}$ where h = Planck's constant, m = mass in grams, v = velocity in m/sec = $1.383 \times 10^4 \sqrt{E(ev)}$, E = kinetic energy = ½ mv^2; $E(ev)$ = kinetic energy in electron volts; λ = wavelength.
Diffraction by crystals	At $E = 1$ ev, $\lambda = 0.286$ A; at $E = 0.026$ ev, $\lambda = 1.8$A: Wavelength in this energy range is of the order of distance between atomic planes in crystals. Bragg diffraction occurs: $n\lambda = 2d \sin\theta$ where n = order of reflection, d = distance between atomic planes, and θ = angle of incidence with plane of atoms.
Interaction with matter	Pass through matter much more readily than charged particles do. Practically no ionization produced. Fast neutrons knock protons from hydrogen-containing material. Prolonged irradiation may change color, thermal conductivity, or electrical conductivity. Bonds may be broken with decomposition of molecules. Due to their magnetic moment, slow neutrons interact with electron magnetic moment of paramagnetic and ferromagnetic atoms.
Detection	Fast neutrons: Recoil protons and nuclear reactions. Example: $\mathrm{Si}^{28}\,(n, p)\,\mathrm{Al}^{28} \xrightarrow[2.3\ \mathrm{min},\ 3.0\ \mathrm{mev}]{\beta^-} \mathrm{Si}^{28}$ Slow neutrons: Radioactivation of foils of In, Mn, Au, Ag, Rh, etc. Example: $\mathrm{Mn}^{55}\,(n, \gamma)\,\mathrm{Mn}^{56} \xrightarrow[1.59\ h,\ 2.8\ \mathrm{mev}]{\beta^-} \mathrm{Fe}^{56}$ Counters lined with B or Li, or proportional counters filled with $\mathrm{B}^{10}\mathrm{F}_3$ Example: $\mathrm{B}^{10} + n \rightarrow \mathrm{Li}^7 + \alpha$ $\mathrm{Li}^6 + n \rightarrow \mathrm{H}^3 + \alpha$ Fission Example: $\mathrm{U}^{235} + n \rightarrow$ high energy fission fragments. Photographic plates containing elements that become radioactive by interaction with neutrons. Scintillation counters arranged to detect γ-rays emitted when neutrons are absorbed or to detect other nuclear reactions caused by neutrons.
Scattering process (n, n) reactions	Elastic nuclear scattering; inelastic nuclear scattering; resonant nuclear scattering; coherent crystal scattering (diffraction); ferromagnetic scattering; paramagnetic scattering; inelastic molecular scattering; neutron-electron scattering.
Absorption process	The neutron is retained by nucleus and a photon or other particle is emitted: (n, γ), (n, p), (n, α). Also $(n, 2n)$ and $(n, \text{fission})$.

Probably the most important and the most widely used method of analysis with neutrons at the present time is that of radioactivation (*3*). Isotope-dilution methods using neutron-produced radioactive isotopes have also proved valuable as a tool for analytical chemistry (*4*). Neutron diffraction (*5*) has supplemented x-ray and electron diffraction in the determination of the structure of an increasing number of substances. Since reviews of the above applications of neutrons to problems in chemistry are already available, this paper will be primarily concerned with those applications that involve the absorption and scattering of a beam of neutrons. In particular, emphasis will be placed upon the change in neutron interactions as a function of their energy or wavelength, as is done in optical spectroscopy.

NEUTRON SOURCES

One of the most important factors involved in the application of neutrons to problems of chemical analysis is the availability of suitable neutron sources. In Table 2 the slow neutron flux obtainable from a number of sources is summarized (*6*). It is to be hoped that future developments will provide the chemist with small laboratory machines for the pro-

---

[1] From a paper presented at the Gordon Conference on Instrumentation, Aug. 1951, and from a general review by the authors in *Nucleonics* (*2*). This work was supported in part by the Atomic Energy Commission, Project AT(30-1) Gen 72.

TABLE 2

NEUTRON SOURCES

Source	Approximate neutron intensity
Chain-reacting piles	
Fission: U^{235} (n, f)	10^{10} to 10^{14} n/cm^2 – sec
Particle accelerators	
Cyclotron: Be^9 (d, n) B^{10}	10^{12} n/sec
Van de Graaf or Cockroft-Walton	$10^8 - 10^{10}$ n/sec
H^2 (d, n) He^3	
H^3 (d, n) He^4	
Li^7 (p, n) Be^7	
Electron linear accelerator	10^{14} n/sec (pulsed)
Be^9 (γ, n) Be^8	
Radioactive (typical sources)	
Radium-beryllium:	
Be^9 (α, n) C^{12}	1.3×10^7 n/Curie-sec
Polonium-beryllium:	
Be^9 (α, n) C^{12}	2.8×10^6 n/Curie-sec
Photoneutron sources:	
Sb^{124} $Be(\gamma, n)$	3.2×10^6 n/Curie-sec

duction of high-intensity neutron sources for certain types of chemical problems.

In practically all sources, the neutrons are liberated at rather high energies (0.1 mev–10 mev) as a result of the nuclear reactions listed in Table 2. Usually, slow neutrons are required for applications to chemical analysis; consequently the fast neutrons must be slowed down. This is done by allowing them to pass through layers of materials containing certain of the lighter elements such as hydrogen (in paraffin or water), beryllium, or carbon. The slowing down results from a billiard-ball–type of collision in which the neutrons lose a part of their kinetic energy to the light element, cascading in a short time to lower energies. A 1-mev neutron, for example, will be slowed down to the thermal energies (0.026 ev) of molecules, on the average, in about 18 collisions with H, 80 with He, 110 with C, and over 2,000 with Pb or U. About 5 cm of paraffin is sufficient for slowing down the fast neutrons.

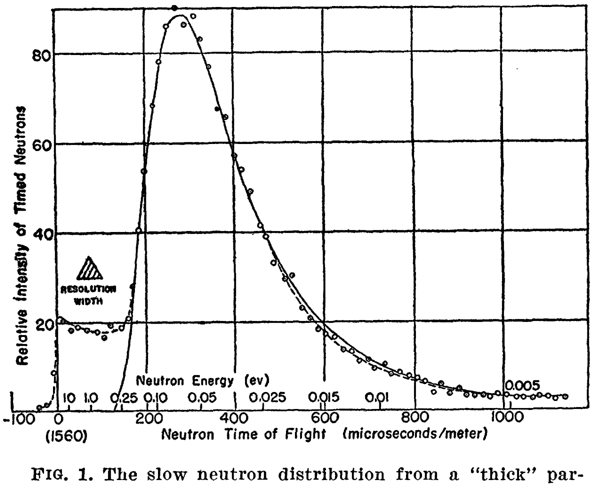

FIG. 1. The slow neutron distribution from a "thick" paraffin source used with the Columbia University cyclotron (6.2-cm thick paraffin in a box of ¼"-thick plywood). Dotted curve follows the experimental points. Solid curve is theoretical for a temperature of 390° K.

The result of the slowing-down process is a flux of slow neutrons that diffuses through the material and emerges with an energy distribution corresponding approximately to the Maxwell-Boltzman distribution for a temperature somewhat higher than the temperature of the slowing-down material. A high-energy component that varies with the source of the neutrons is also present. A typical energy or wavelength distribution of slow neutrons produced in this way is illustrated in Fig. 1.

In some of the applications that will be described later, slow neutrons with a rather broad energy distribution are useful. However, if the interactions at a particular energy or wavelength are to be used for a chemical analysis, it is necessary to select a narrow energy band by means of suitable spectrometers, velocity selectors, filters, or selective detectors.

NEUTRON SPECTROMETERS

Mechanical velocity selectors. One of the first methods of selecting a narrow energy band of neutrons employed a mechanical velocity selector and was used by Dunning, Pegram, Mitchell, and Segre (*7*) in conjunction with a radium-beryllium source. Other types of mechanical velocity selectors (*8*) have been designed since that time for operation in different regions of the slow neutron distribution curve. The general principle of the mechanical velocity selector, when used as a neutron spectrometer, is illustrated in Fig. 2. It was designed by Fermi and his co-workers (*8*) for use with the chain-reacting pile. A rotating cylinder of alternate thin laminations of aluminum and cadmium is placed next to the graphite thermal neutron column. Neutrons can pass through the cylinder only when the direction of the layers is parallel to the beam. The mirror rotates with the cylinder, and the reflected light activates the photoelectric tube, which in turn activates the BF_3 neutron counter. By adjusting the position of the mirror, the photoelectric tube and counter can be activated at time t after the neutrons have passed through the cylinder. Thus only those neutrons are counted whose velocity is equal to d/t. An absorber can then be placed in the beam, and the transmission of neutrons through it for this velocity can be measured. The time t can then be changed, and the transmission can be measured at other velocities. This method is useful to about 0.2 ev, where the resolution becomes poor because the speed at which the cylinder can be rotated is limited.

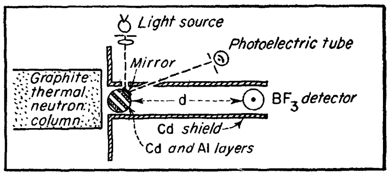

FIG. 2. Schematic diagram of a mechanical velocity selector.

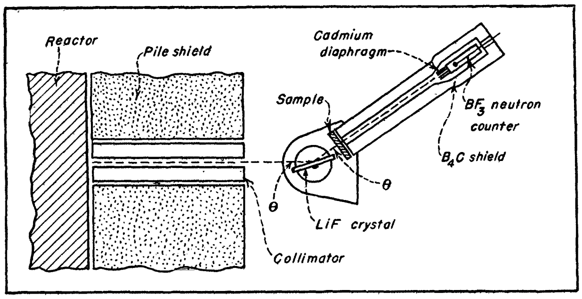

FIG. 3. Schematic diagram of a crystal spectrometer for neutrons.

The mechanical velocity selector designed by Selove (*9*) is useful for the higher energy neutrons (short wavelengths), whereas the one devised by Hughes (*10*) and his co-workers is useful in the lower energy regions (long wavelengths to about 20 A).

Crystal spectrometer. Crystal spectrometers for selection of neutrons of a narrow energy-band or wavelength range are based on the wave properties of neutrons (*11*). The general arrangement of the equipment as illustrated in Fig. 3 is very similar to that used for x-ray spectrometers.

Neutrons from a chain-reacting pile are collimated so that a parallel beam of neutrons hits the surface of a crystal such as lithium fluoride. Maxima in the diffraction pattern occur in such a way that the Bragg relation $n\lambda = (nh)/(mv) = 2d \sin \theta$ is satisfied (Table 1). Neutrons of a given energy can be obtained by setting the crystal and detector at the appropriate angle with respect to the neutron beam. Thus, if the (100) planes of LiF in which $d = 2.005$ A are set such that $\theta = 20$ degrees, then the velocity of the neutrons impinging upon the crystal can be calculated in the following manner for a first-order reflection:

$$v = \frac{nh}{m\,2d \sin\theta} = \frac{(1)(6.62 \times 10^{-27})}{(1.67 \times 10^{-24})(4.01 \times 10^{-8})(0.342)} = 2.88 \times 10^{5} \text{ cm/sec},$$

which corresponds to an energy in electron volts of

$$E = \frac{\frac{1}{2} mv^2}{e} = \frac{(0.5)(1.67 \times 10^{-24})(2.88 \times 10^{5})^2 (300)}{4.80 \times 10^{-10}} = 0.0430 \text{ ev}$$

or to a wavelength of $\lambda = h/(mv) = 1.38 \times 10^{-8}$ cm, or 1.38 A.

To measure the transmission of a sample at this velocity, the intensity of the beam is measured, first without the sample present and then with the sample between the crystal and the detector. The angle of incidence, θ, can then be changed to obtain the transmission at other neutron energies from 0.01 to 100 ev. At the higher energies the angle of incidence is very small, and at lower energies the higher-order reflections interfere. One important advantage of the crystal spectrometer is that the beam is essentially monoenergetic; that is, the only neutrons that pass through the sample are those that have the energy given by the Bragg equation. Consequently, by measuring the activation of the sample, the cross section of certain isotopes can be determined.

Time-of-flight velocity selector. Block diagrams showing the general principles of the modulated cyclotron velocity selector (*12*) are given in Figs. 4 and 5. By modulating the ion-accelerating potential in the source of a cyclotron, short bursts of deuterons can be made to hit a beryllium target. This produces fast neutrons for short periods of τ μsec (variable from 2 to 1,024 μsec) in the Columbia University neutron spectrometer. After being slowed down in paraffin, they travel toward the detector placed at a distance d (6 m) from the source. The neutrons arriving at the detector after t_1 μsec (except for a small correction for the time necessary to accelerate the deuterons and to slow down the neutrons) are counted for a period of τ′ μsec. This period is usually the same as the time of the neutron burst.

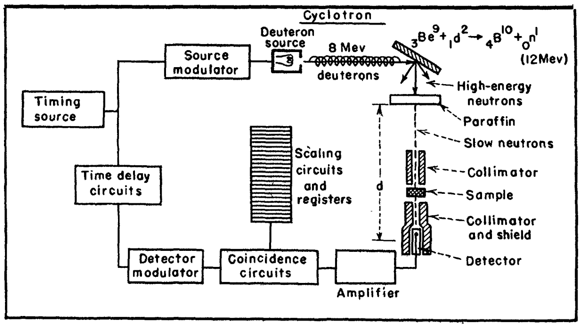

FIG. 4. Block diagram of cyclotron velocity selector.

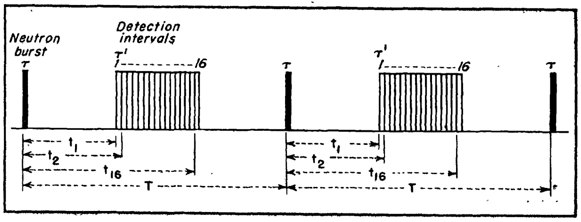

FIG. 5. Principle of the time-of-flight velocity selector.

The time-of-flight of this group of neutrons is then t_1/d μsec/m, or their velocity is d/t_1. At the end of this first detection interval, a second coincidence unit is turned on for τ μsec to count the neutrons arriving after a time of t_2 μsec. In this way, a total of 32 scaling units count the neutrons arriving at the detector during each of the 32 successive detection intervals of τ μsec each.

After a time T—which may be 1,024 μsec, for example—another burst of neutrons is produced, and the neutrons are again counted at each detection interval. The time between bursts can be adjusted in steps from 256 to 32,768 μsec, and the detection may be started at any delay time t_1 after the start of the burst. Also, both the duration of the burst τ and of the detection interval τ′ can be varied from 2 to 1,024 μsec. With this system, the number of neutrons arriving at the detector as a function of time can be determined in any desired range of neutron energies from 0.001 to 10,000 ev. The resolution is approximately triangular and constant for a specified setting of the apparatus, when measured on the time-of-flight basis.

The general arrangement of the cyclotron is shown diagrammatically in Fig. 6. Neutrons emerging from the paraffin source are collimated by thick shields of boron carbide. They then pass through the sample, and into the detector, which consists of a proportional counter 10 cm long and 5.0 cm in diameter, filled with 50 cm of BF_3 enriched in B^{10}. Actually, two channels with associated detectors, circuits, and scaling units are provided. By alternating the container plus sample with an identical empty container between the two channels, duplicate determinations of the transmission can be obtained. An average of the values obtained in this way improves the accuracy of the transmission measurements by reducing the effects of fluctuations in the intensity of the neutron beam. The effects of fluctuations are also minimized by counting the neutrons arriving at the counters for equal amounts of total neutron production rather than for equal intervals of time. A uranium fission-chamber placed within the cyclotron enclosure is used for this purpose. Detailed discussion of the operation of the cyclotron velocity selector is given in papers by Rainwater, Havens, Wu, Dunning, and their associates (*13*).

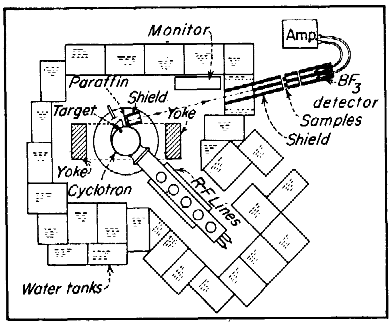

FIG. 6. Geometrical arrangement of cyclotron velocity selector, samples, and detector.

Resonance detectors and filters. Resonance detectors (*14*) combined with suitable filters may at times be conveniently employed to measure transmissions of samples at the resonance energy of the detector. For example, the transmission of a substance for neutrons with an energy of 1.45 ev (the resonance absorption energy for indium) can be measured using indium foil surrounded by cadmium as a detector. The radioactivity induced in the foil with the sample in the beam, divided by the radioactivity induced in the foil with the sample out of the beam, gives the transmission of the sample at this energy. Other resonance detectors besides indium, such as thin foils of gold, silver, or manganese, etc., can be used.

From the radioactivity induced in the detector foil by the (n, γ) reaction, the intensity of the beam can be calculated, as will be described later. By placing a cadmium filter in front of one of these detector foils, thermal neutrons are removed, and the foil is activated primarily by neutrons of an energy corresponding to the resonance energy of the foil element. This makes it possible to determine the transmission for a rather sharply defined energy group of neutrons. Indium, for example, has a resonance at 1.45 ev, gold at 4.87 ev, iodine at 40 ev, cobalt at 126 ev, and manganese at 335 ev.

If more than one activation resonance is present in the detector, then one or another of the levels can be discriminated against by using the proper boron or cadmium filter. Although this method has certain limitations, it can be useful in determining the transmission at a particular energy when a velocity selector is not available. Cross sections for indium resonance neutrons have been tabulated by Marshall (*15*) and by Hanstein (*16*), and can be used for the determination of composition, as will be described later.

A radium-beryllium source with which these detectors may be used in a laboratory is illustrated in Fig. 7. Neutron sources of this or other types (Table 2) can be arranged for transmission experiments using either the radioactivation of foils or BF_3 counters. Samples can also be introduced for radioactivation analysis.

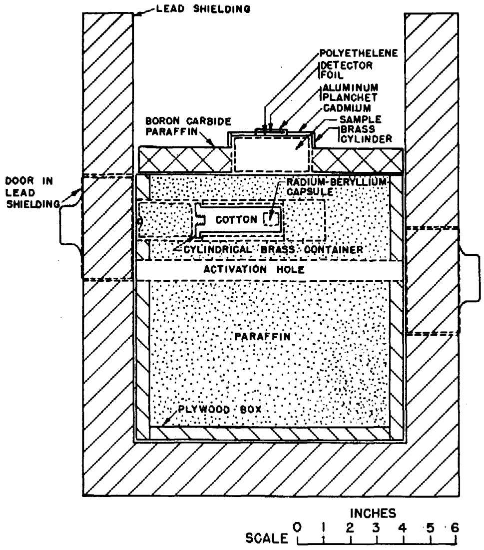

FIG. 7. Vertical sectional view through the center of a ½ Curie radium-beryllium source for using resonance detectors. A 4″-wall of lead and a 1/16″-sheet of cadmium in front of the source is used for protection against radiation.

Use of cadmium and other filters. For certain analyses, particularly those in which the sample contains elements that have resonance peaks near the thermal region, it may be advantageous to change the energy distribution of the beam with appropriate filters. Cadmium filters can, for example, be used to obtain the transmission for neutrons below 0.4 ev. Since cadmium has a strong absorption resonance at 0.180 ev, a thickness of about 0.6 mm removes practically all neutrons with energies below 0.4 ev. The neutrons not transmitted by such cadmium filters are called c neutrons.

By making measurements with and without a cadmium filter, transmissions can be obtained for neutrons with energies above and below the cadmium cutoff. Four measurements are required:

1) Open beam intensity, I_o
2) Intensity with the sample in the beam, I_{sample}
3) Intensity with the cadmium filter in the beam, I_{Cd}
4) Intensity with both cadmium filter and the sample in the beam, $I_{\text{Cd+sample}}$

The transmission T_e for the e neutrons is

$$T_c = \frac{(I_{\text{sample}} - I_{\text{Cd+sample}})}{(I_o - I_{\text{Cd}})} \qquad (1)$$

and the transmission T_{ec} for the neutrons with energies above the cadmium cutoff—i.e., epi c neutrons—is given by

$$T_{ec} = \frac{I_{\text{Cd+sample}}}{I_{\text{Cd}}} \qquad (2)$$

These transmission values can then be used as will be described later for determining the composition of the sample.

Another filtering material that has been particularly useful in neutron measurements is boron, because the cross section is known to be directly proportional to $1/v$ or $+1/\sqrt{E}$. By means of boron filters of different thicknesses, the energy distribution of the neutron beam can be changed. The thicker the boron filter, the higher the average energy of the neutron beam. In this way, the cross section of a sample for different average energy distributions may be determined.

Thermal neutron beam. For application to certain simple systems it is not necessary to select a narrow energy band of neutrons. Instead the rather broad energy band of neutrons slowed down in paraffin can be used (Fig. 1). This distribution varies somewhat with the source of neutrons and with the temperature of the paraffin, but the observed transmissions are effectively those for neutrons of an energy of about 0.04 ev. Applications of this method to cases where one element in a mixture has a high cross section for thermal neutrons will be described later.

CROSS SECTIONS FOR NEUTRON INTERACTIONS

The magnitude of neutron interactions is usually expressed in terms of "cross sections." The unit is the barn (1×10^{-24} sq cm), which is of the order of physical area of nuclei. Cross sections for many reactions can be measured by transmission experiments as discussed in the following.

When an essentially unidirectional beam of neutrons is incident on a sample of material, some of the neutrons pass through unaffected, and the others are either absorbed or scattered from the beam as a result of neutron interactions. This attenuation of the neutron beam can be determined in a suitable experimental arrangement, shown diagrammatically in Fig. 8. The fractional decrease in intensity dI/I_x of a neutron beam in passing through a layer dx (Fig. 8) is equal to the ratio of the effective area of the nuclei in the layer to the total area of the layer. The effective area presented by the nuclei is given by the total effective cross section σ_t of each nucleus times the number of nuclei in the layer or $\sigma_t\, n\, A\, dx$, where n is the number of nuclei per cc and A is the area. Hence

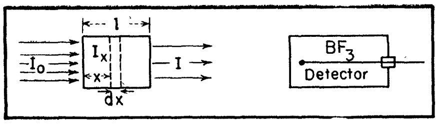

FIG. 8. Neutron cross sections from transmission measurements: I_o = initial neutron intensity; I_x = neutron intensity at x; l = thickness of sample.

$$dI/I_x = -\sigma_t\, n\, A\, dx/A = -\sigma_t\, n\, dx, \text{ from which}$$
$$I = I_o e^{-\sigma_t nl} \qquad (3)$$

where I_o is the initial intensity of the neutron beam, and I is the intensity after it has passed through the sample of thickness l. Hence, the total cross section per nucleus in cm² can be calculated from the results of transmission measurements by using Eq. (3) in the form

$$\sigma_t = \frac{1}{nl} \ln \frac{I_o}{I} = \frac{1}{nl} \ln \frac{1}{T}. \qquad (4)$$

Since the number of atoms per cc is given by $\rho N/M$, where M is the atomic weight, ρ is the density, and N is Avogadro's number,

$$\sigma_t = \frac{M}{\rho N l} \ln \frac{I_o}{I} = \frac{M}{\mu N} \ln \frac{I_o}{I}, \qquad (5)$$

in which μ is the grams per square centimeter of the element in the path of the neutron beam.

The cross section obtained in this way is the total cross section for all processes that tend to deflect the neutrons from their straight line of flight. Charged-particle scattering measurements and the lifetime energy relationship in heavy-charged-particle emitters indicate that the actual physical radius of an element of mass number A is given approximately by $1.5 \times 10^{-13} \times A^{1/3}$. For an element of mass number of about 125, the radius of the nucleus would be 7.5×10^{-13} cm, or a cross section of about 1.8×10^{-24} cm² (1.8 barns). Cross sections for neutrons may vary from this value up to over 115,000 barns for gadolinium at a neutron velocity corresponding to an energy of about 0.002 ev; that is, the cross section of this nucleus at certain energies is many thousands of times larger than its actual physical cross section. Since the observed cross sections depend so markedly upon the velocity of the neutrons, it becomes necessary to examine more closely the processes that contribute to the cross section.

NATURE OF NEUTRON INTERACTIONS

One of the generally adopted views of nuclear interactions is based upon Bohr's (*17*) idea of the compound nucleus, as illustrated in Fig. 9. On the basis of this picture, a neutron that comes close enough to a nucleus to interact with it actually unites with it to form a compound nucleus. This new nucleus, excited by both the kinetic energy of the neutron and by the

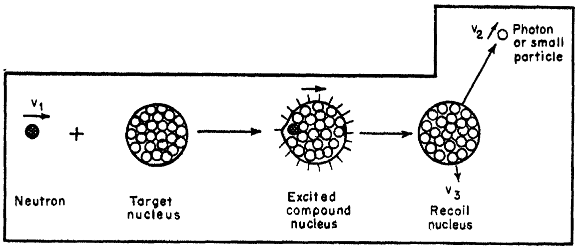

FIG. 9. Interaction of a neutron with a nucleus.

binding energy of the neutron with the nucleus (8–9 mev), may change to a more stable state in any one of a variety of ways. The relative probabilities for the different possible reactions are usually described in terms of "reaction widths," $\Gamma\chi$. The total cross section σ_t obtained from transmission measurements is the sum of the cross sections for all the absorption and scattering interactions summarized in Table 1. Thus the total cross section for transmission of crystals for slow neutrons will be given by

$$\sigma_{\text{total}} = \sigma_a + \sigma_{el} + \sigma_{inel} + \sigma_{coh} + \sigma_D + \sigma_m + \dots, \quad (6)$$

in which the terms refer respectively to cross sections arising from absorption, elastic, inelastic, coherent Bragg scattering, diffuse or incoherent effects, and magnetic effects.

Absorption. Except for a few of the lighter elements, the most probable absorption reaction for slow neutrons is the (n, γ) reaction, in which the incident neutron is retained by the nucleus and a photon (γ) is emitted. This reaction is sometimes called radiative capture, because the γ-ray is emitted from the compound nucleus very shortly after it is formed (about 10^{-14} sec). The atomic number does not change in this process, but the mass number increases by one unit. If the isotope does not normally exist in nature, it will be radioactive. The properties of many of the radioactive isotopes formed in this way are suitable for chemical analysis by the radioactivation method.

Scattering. When a neutron rather than another particle is emitted from the compound nucleus, scattering results, and the process is called an (n, n) reaction. For most of these reactions neutrons are emitted nearly isotropically from the compound nuclei, and, consequently, very few of them reach the detector if good geometry is maintained. For good geometry the incident neutron beam should be essentially parallel, and the detector should be sufficiently distant from the sample that it subtends only a negligible solid angle.

Scattering may be inelastic if a part of the kinetic energy is lost by a fast neutron in exciting the nucleus to higher energy levels. Slow neutrons may also be involved in inelastic molecular collisions when a part of their kinetic energy is used up in breaking bonds or in exciting higher vibrational and rotational energy states of molecules or crystals.

Elastic-type collisions occur when the kinetic energy of the neutron and nucleus remains constant, and the interaction may be treated as a billiard-ball-type of collision. This is the main process by which fast neutrons are slowed down by the lighter elements.

When the energy or wavelength of the neutron is decreased to the thermal region where the associated wavelength is of the order of the distance between atoms in crystals, diffraction effects occur (*5*) in accordance with the Bragg relation, $n\lambda = 2d \sin\theta$. With a heterogeneous beam of neutrons Laue patterns may be obtained, whereas with a monoenergetic or monochromatic beam powder patterns can be taken with a neutron spectrometer. The intensity of the coherently scattered neutrons depends upon scattering from nuclei, but x-ray scattering involves the electrons of the atoms, and therefore depends markedly upon the atomic weight of the element. Neutron scattering, on the other hand, is about as intense for the nuclei of light atoms as for heavy atoms. For example, the relative coherent scattering cross sections in barns for a few elements are: $H = 1.8$, $D = 5.4$, $O = 4.2$, $Na = 1.5$, $Cu = 7.3$, $Bi = 9.4$. This makes possible the determination of the position of hydrogen in crystals by neutron diffraction where it would not be possible by x-ray diffraction. If the absorption cross section is large for one or more of the elements in a crystal, the intensity of the beam may be reduced so much that neutron diffraction will not be very useful.

Differences between neutron diffraction and x-ray diffraction also occur with respect to *diffuse scattering* effects that arise from such things as differences in the *scattering amplitude* and the *spin* of the isotopes of the element. Some elements, such as H^1, Li^6, Ti, and Mn, scatter neutrons with a *phase* opposite to that of D, Li^7, and most other elements (*5*). Consequently the amplitude of the scattered wave from planes in crystals containing nuclei of opposite scattering phase will be reduced. This effect is useful in certain structure problems, particularly those involving hydrogen, where both the hydrogen and deuterium compounds can be studied.

When the energy of the neutrons is reduced to a value such that the wavelength is equal to $2d$ for the first Bragg reflection, no coherent crystal scattering will occur. Neutrons of longer wavelength can then readily pass through the crystals. This effect has been used to obtain neutron beams of long wavelength by filtering through BeO (*18*). With such a filter, neutrons with wavelengths less than about 4.5 A are scattered from the beam. The residual cross section for the longer wavelengths is then caused by absorp-

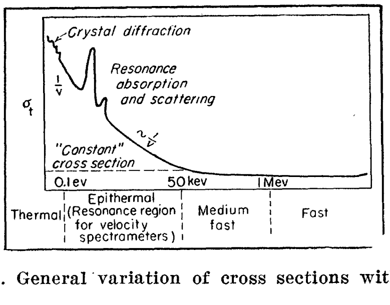

FIG. 10. General variation of cross sections with neutron energy.

tion, inelastic molecular effects, crystal imperfections, spin, isotope, temperature effects, etc. In addition, paramagnetic (*19*) and ferromagnetic substances have an additional effect caused by the interaction of the nuclear magnetic moment of the neutron and the electron magnetic moment of the unpaired electrons. Paramagnetic scattering becomes important only at the lower energies (long wavelengths).

Variations in Cross Sections with Neutron Energy

Marked variations exist in the cross sections for neutron interactions as the velocity of the neutron is changed. At high energies (1 mev), where the wavelength of the neutron is of the same order of magnitude as the radius of the nucleus ($\lambda \approx R$), the effective total cross section is roughly twice the geometric size of the nucleus or $2\pi r^2$ as measured by other methods—i.e., from 1 to 10×10^{-24}cm² (1–10 barns). In this high-energy region, the principal processes involve particle emissions, primarily scattering [(n, n) reactions]. However, there are some (n, p) and (n, α) reactions. As the energy of the neutrons is decreased, the cross section increases approximately as $1/v$, as illustrated in Fig. 10.

Resonance absorption and scattering of slow neutrons. Many of the elements, particularly those with atomic masses above 100, show regions of resonance absorption and scattering where a marked increase in cross section occurs at definite neutron energies (Fig. 10). One or more of these resonances exist for many nuclei. The fact that they occur at specific neutron energies may serve as an indication of the presence or absence of a particular nuclear species in an unknown sample. Furthermore, the large cross section at resonance is useful in quantitative determinations of a limited number of elements, some of which can be determined chemically only with difficulty. Examples will be given in a later section.

The shape of the resonance curve is given by the Breit-Wigner formula (*1*). The cross section at an energy E (electron volts) in the region of a resonance for an (n, γ) reaction is:

$$\sigma_{(n,\ \gamma)} = \frac{\lambda^2}{4\pi}\, g\, \frac{\Gamma_n \Gamma_\gamma}{(E - E_o)^2\, (\Gamma/2)^2} \qquad (7)$$

where λ is the wavelength [$\lambda = h/(\mathrm{mv})$] of the incident neutron, and g is a statistical weight factor for the spins of the target nucleus, the compound nucleus, and the neutron. $\Gamma\gamma$ is the partial level width (proportional to the reaction probability) of the (n, n) process. It is convenient to include the value of g in this neutron width. $\Gamma\gamma$ is the partial level width with respect to the (n, γ) process. $\Gamma = \Gamma n + \Gamma\gamma$ is the full width of the resonance peak at half its maximum value σ_o. E is the energy of the incident neutron, and E_o is the resonance energy.

For low-velocity neutrons, $\Gamma\gamma$ is nearly independent of velocity, whereas Γn is proportional to v. The maximum possible cross section for the (n, γ) process would be

$$\sigma_{o(n,\ \gamma)} = \frac{\lambda^2}{\pi} \cdot \frac{\Gamma_n \Gamma_\gamma}{\Gamma^2}, \qquad (8)$$

or $\lambda^2/4\pi$ at $E = E_o$ if $\Gamma n = \Gamma\gamma$. This would be a possible total cross section of $\lambda^2/2\pi$ for the sum of both $\sigma_{o(n,\ \gamma)}$ and $\sigma_{o(n,\ n)}$. A few nuclei such as Pd^{108}, Sm^{152}, and W^{186} appear to have levels in which $\Gamma\gamma \approx \Gamma n \approx 0.1$ ev.

Resonance capture. In most cases, however, $\Gamma n < \Gamma\gamma$ by a factor of 10 to 100, so that $\Gamma\gamma \cong \Gamma$ and the maximum possible cross section for resonance absorption is $\sigma_o = \lambda^2/\pi(\Gamma n/\Gamma\gamma)$. Since Γn varies as the velocity v or as $\sqrt{E}$, the cross section $\sigma_{(E)}$ for an energy E other other than the resonance energy can be obtained by bringing Eq. (7) into the following form:

$$\sigma_{(E)} = \left(\frac{E_o}{E}\right)^{1/2} \frac{\sigma_o \Gamma^2}{4(E - E_o)^2 + \Gamma^2} \qquad (9)$$

At energies low compared to E_o, Eq. (*9*) shows that $\sigma_{(E)}$ is proportional to $1/\sqrt{E}$ or to $1/v$. This is the well-known $1/v$ law. Examples of the above are Rh^{103}, In^{151}, and Au^{179}, in which $\Gamma\gamma$ is about 0.1 ev compared to 0.001 ev for Γn.

Resonance scattering. The cross section $\sigma_{(n,\ n)}$ for elastic scattering of low-energy neutrons in the region of a resonance is

$$\sigma_{(n,\ n)} = \frac{\lambda^2}{\pi} \times \frac{\Gamma_n^2}{4(E - E_o)^2 + \Gamma^2}, \qquad (10)$$

which, at the resonance energy E_o, gives a maximum cross section of λ^2/π. There are cases of levels, such as in Mn and Co, in which scattering is the more favored process, $\Gamma n \approx 10$ ev and $\Gamma\gamma \approx 0.1$ ev.

The 1/v region. At low energies, the cross section for scattering varies as $(\lambda^2/\pi) \times (\Gamma^2 n/4E_o^2)$, and

TABLE 3

Constants for the $1/v$Region for a Number of Elements
(Equation: $= a + b/v = a + c/\sqrt{E}$)

Element	a Constant scattering cross section	c Slope
Ag	6.6	9.05
Al	1.48	0.036
Au	12.4	14.5
B	3.8	113.0
C	4.8	0.0007
Co	6.7	6.4
Cu	7.8	0.54
F	4.0	0.0016
Fe	11.1	0.34
Hf	84.6	38.7
In	14.0	64.5
Li	1.5	11.5
Mn	2.26	2.24
Nb	6.4	0.10
Nd	14.4	14.6
Ni	17.0	0.77
O	3.7	< 0.0001
Rh	6.0	23.6
Sn	4.3	0.088
Ta	7.2	3.2
W	5.7	2.72
Zr	6.8	0.016

since λ varies as $1/v$ and Γn varies as v, the scattering cross section should be fairly constant. Hence, the total cross section $[\sigma_{\text{total}} = \sigma_{\text{capture }(n,\gamma)} + \sigma_{\text{scattering }(n,n)}]$ in the $1/v$ region is made up of a constant scattering term plus a capture term that varies as $1/v$ or as $1/\sqrt{E}$. Thus, the cross section in this region can be expressed by an equation of the form $\sigma_{(E)} = a + b/v$ or $\sigma_{(E)} = a + c/\sqrt{E}$. The magnitudes of the absorption cross sections in this region, as well as the slopes of the $1/v$ curves, differ for a number of the elements (Table 3 and Fig. 11). Consequently, a method of analysis of certain simple systems can be based upon the transmission at two different neutron velocities. This method would give adequate precision only in cases where the $1/v$ slopes are markedly different for the elements in the sample.

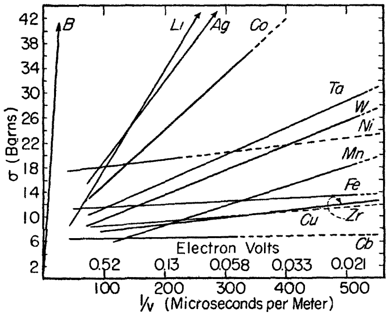

FIG. 11. Typical $1/v$ lines for several elements.

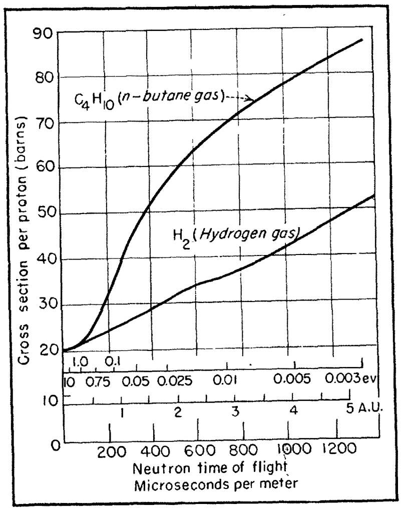

FIG. 12. Graph of neutron cross section n-butane and hydrogen as a function of neutron energy. (Approximate corrections have made for translational motion.)

Molecular effects. In the case of the lighter elements, such as hydrogen and deuterium, chemical binding effects become significant below energies of 1 ev. Actually the scattering is proportional to the square of the reduced mass of the neutron and the scatterer (*1*). If the hydrogen atom is free, the reduced mass $\mu \cong 0.5$. However, when hydrogen is bound in heavy molecules such as paraffin, the reduced mass will be $\mu \cong 1$. Consequently the ratio of the cross section of the free hydrogen atoms to a rigidly bound one is approximately $(1/0.5)^2 = 4$. Or, in general, the cross section σ_b for a rigidly bound nucleus of mass A relative to the cross section σ_f of the same nucleus in a free state will be given by $\sigma_b = \sigma_f[A+1)/A]^2$.

When the energy of the neutron is considerably higher than the vibrational energy of the C—H bond in paraffin (i.e., $E >> h\nu \approx 0.4$ ev), H may be separated from the molecule, and the cross section for hydrogen is what would be expected for free hydrogen atoms. At energies of the order of $h\nu$, however, the neutron can lose energy to the vibration of the hydrogen atom or other groups in the molecule. In this case the hydrogen atom is essentially bound, and the cross section increases to about four times that at the higher energies. Experiments show, in fact, that the cross section for hydrogen bound in a hydrocarbon molecule does increase from about 20 barns in the region of 10–1 ev to over 80 barns at energies of about 0.005 ev, as shown in Fig. 12 (*21*).

These results indicate that thermal neutrons (0.026 ev) would be quite suitable for analyzing certain materials for hydrogen-containing compounds. Specific applications of thermal neutrons to such analysis will be considered later. Also, it appears that such cross-section curves plotted as a function of energy may give some useful information on the absorption and combination of hydrogen with metals.

ANALYSIS BY RESONANCE ABSORPTION AND SCATTERING OF NEUTRONS

Neutron absorption and scattering resonances are characteristic of a particular nucleus and therefore can be used to analyze for the presence of that nucleus. The cross section vs. energy curve for tantalum shown in Fig. 13 is typical of the experimental results obtained for many of the elements. As shown in this curve, tantalum has a large resonance absorption at 4.1 ev. This can be used not only to indicate the presence of tantalum but also to measure quantitatively the amount of tantalum in a sample that contains no elements with interfering resonances. It is, for example, useful in determining the percentage of tantalum in a sample of columbium. Similar curves have been obtained and compiled for many of the elements (*22*).

The principal resonances for a number of the elements are given in Table 4. Those elements with large cross sections can be detected qualitatively and determined quantitatively in the absence of elements with interfering resonances or high cross sections in the regions of the resonances; consequently it is necessary to have some knowledge of the nature of the samples. Resonances for the lighter elements (atomic weights below 100) occur only at relatively high energies, where the velocity selectors described previously are not very useful.

Examples of cases where analyses appear to be feasible are: Ta in Nb; Hf in Zr; In in Sn; Mn in Al or Fe; Co or Mn in steel; the rare earth elements; and

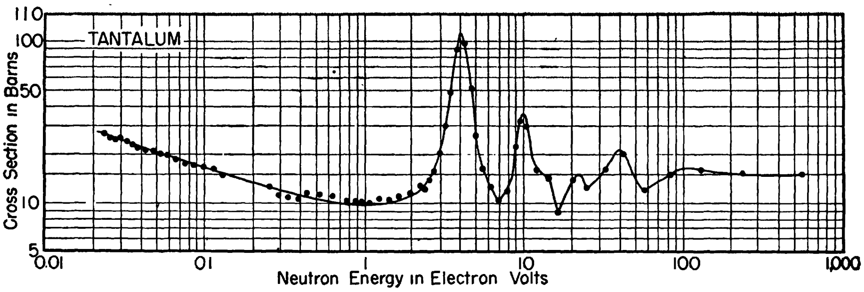

FIG. 13. Slow neutron cross-section curve of tantalum.

thicknesses of films or electroplates of Ag, Au, Rh, or Cd. The analysis can be done by obtaining an empirical working curve from a series of appropriate standards, just as is done in analysis by light absorption, or it can be done from a single curve, if the Breit-Wigner constants for the resonance curve of the element are known. This is illustrated in the following section by the case of hafnium impurity present in zirconium.

In Fig. 14 the transmission as a function of neutron energy is given for a sample containing 160. mg/cm^2

TABLE 4

SLOW NEUTRON RESONANCES

Element	E_0ev	$\sigma\Gamma^2$ barns (ev)^2
Antimony	5.8	12
	15.	35
	21.	35
Bromine	35.7	220
	54.	140
	104.	250
	136.	1000
Cadmium	0.176	828
Chromium	3950.	61.5×10^6
Cobalt	126.	2.3×10^5
	5500.	—
	8000.	—
Copper	3000.	—
Dysprosium	1.9	100
	5.	300
Europium	0.5	500
	3.	700
	10.	400
	25.	300
Gadolinium	0.04	90
Gallium	100.	846
	296.	4.92×10^4
Germanium	95.	800
Gold	4.87	638
Hafnium	1.07	38
	2.37	—
	5.5	—
	7.3	—
Indium	1.45	210
	3.8	12
	8.6	30
Iodine	20.6	4
	32.	135
	42.	135
Iridium	0.64	5 to 20
	1.27	5 to 20
	5.2	55
	8.7	50
	25.	—
Iron	950.	—
Manganese	335.	1.4×10^6
	2800.	—
	8400.	—
Mercury	−2.0	—
Osmium	6.5	10
	8.8	35
	20.	25
	28.	8
	42.	10
	84.	—
Platinum	11.5	55
	18.2	30
	100.	—
	1000.	—
Rhenium	2.2	46
	4.4	67 ($\sigma_0\Gamma$)
	5.9	24 ($\sigma_0\Gamma$)
	7.2	91 ($\sigma_0\Gamma$)
	11.3	30
	13.1	45 ($\sigma_0\Gamma$)
	16.7	46
	21.1	120 ($\sigma_0\Gamma$)
Rhodium	1.27	150
Ruthenium	9.8	11
	15.2	11
	24.1	16
	40.9	29
Samarium	0.10	50
	10.	200
Silver	5.1	300
	15.9	23
	29.6	—
	39.7	—
	51.	—
	66.	—
	84.	—
	93.	—
Sodium	3000.	—
Tantalum	6.1	—
	10.3	44
	13.6	9
	20.	9
	24.	35
	35.	97
	39.	197
Thallium	1300.	9×10^5
Tungsten	4.0	13
	7.4	5
	18.0	3000
	45.	400
	180.	1000
	1100.	
Zinc	520.	6.9×10^4
	1100.	2.3×10^4
	3800.	2.5×10^6

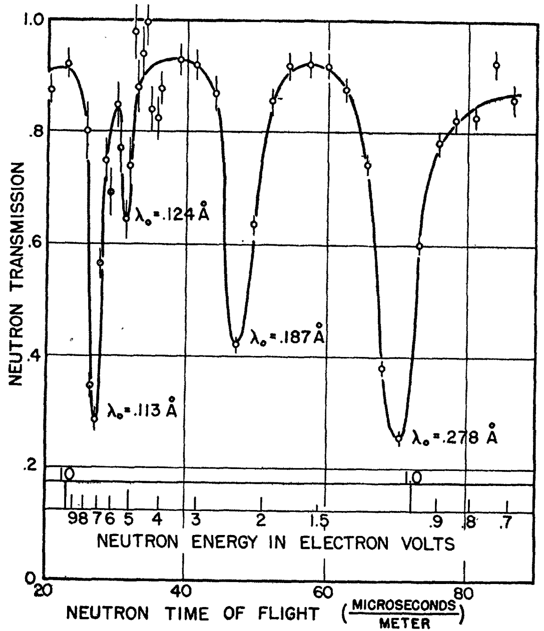

FIG. 14. Slow neutron transmission of a sample of hafnium (160 mg/cm²).

of hafnium. A section of a similar curve is given in Fig. 15 for a sample of zirconium, 16.3 g/cm². It is obvious from these curves that the resonances in the zirconium sample occur at about 47 and 70 μsec/m, or 2.37 and 1.07 ev, the same as resonances in the sample of hafnium. Resonance absorption at this energy is characteristic of the hafnium nucleus and can be used as a qualitative identification of this element. The following treatment will show how the area of this resonance dip can be used for quantitative estimation, once the appropriate constants are known for the element.

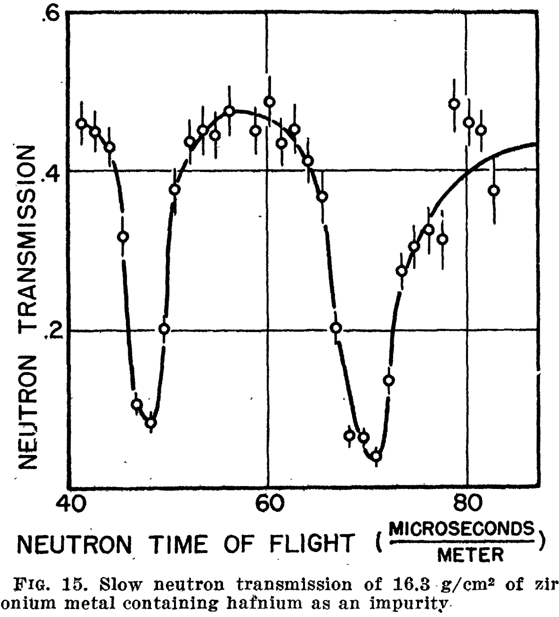

FIG. 15. Slow neutron transmission of 16.3 g/cm² of zirconium metal containing hafnium as an impurity.

When the energy of the neutron is not near the resonant energy of any of the isotopes present, the cross section is approximately $4\pi r^2$ where r is the nuclear radius. This cross section varies between 2 and 11 barns for practically all elements. When the energy of the neutron approaches the resonant energy, the cross section increases very rapidly. In some cases, it may become as high as 1,000,000 barns at E_0. This rapid increase in cross section in the vicinity of a resonance causes the resonant dip in the transmission curve.

In the transmission curve for a sample of material, the observed transmission near a resonance can be divided into two parts: (*a*) the part which is due to the resonance absorption and scattering of a particular isotope and which changes rapidly with energy, and (*b*) the part which represents the sum of the elastic scattering cross sections of all nonresonant nuclei present and which does not vary rapidly with energy. Since one part of the cross section does, and the other part does not, vary rapidly with the energy, this "background" transmission (the part that does not vary rapidly with energy) can usually be obtained without difficulty.

It is obvious from the transmission curve of zirconium with the hafnium impurity that the hafnium transmission dip recovers to the background transmission of approximately 0.49. A derived "resonance transmission curve" for the hafnium in this sample of zirconium can be obtained by dividing the observed transmission curve by the background transmission. This derived transmission curve is the one used for the quantitative estimation of an element.

Effect of resolution width. To obtain the quantity of an element from its resonance transmission curve, one must consider the method by which the data are obtained.

In the modulated cyclotron velocity selector, as described above, there is approximately uniform production of neutrons for a time τ and detection of the neutrons for an interval of time τ'. Suppose for simplicity (and usually applied in practice) that we let $\tau = \tau'$. Then neutrons having times-of-flight between $t_1 - \tau$ and $t_1 + \tau$ will be detected and recorded. The probability that the particle having a time-of-flight t between $t_1 - \tau$ and $t_1 + \tau$ being detected will be proportional to the sum of area of the production pulse and the detection pulse overlapping at the time t. Therefore, the probability of a particle of time-of-flight t being detected will be zero at $t = t_1 - \tau$, increase linearly until $t = t_1$, and then decrease linearly to zero at $t = t_1 + \tau$.

The probability of detection can be represented mathematically by a distribution function expressed by the following relations:

$$\Phi(t, \tau) = 0 \text{ for } t < (t_1 - \tau)$$
$$\Phi(t, \tau) = \frac{1}{\tau^2}\,[t - (t_1 - \tau)] \text{ for } (t_1 - \tau) < t < t_1$$
$$\Phi(t, \tau) = \frac{1}{\tau^2}\,[(t_1 + \tau) - t] \text{ for } t_1 < t < (t_1 + \tau)$$
$$\Phi(t, \tau) = 0 \text{ for } t > (t_1 + \tau)$$

This distribution function is usually called the resolution function or resolution width of the apparatus. The relation of the resolution function of the apparatus to "cyclotron on time" and "detector on time" is given in Fig. 16.

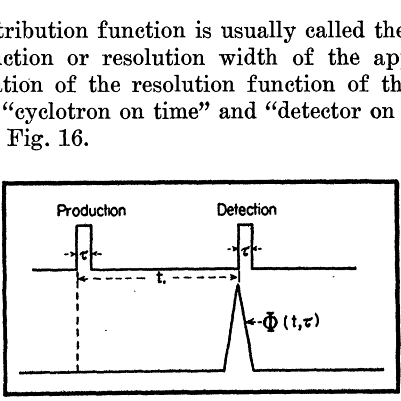

FIG. 16. Resolution function of the apparatus $\phi(u)$ showing relation to "cyclotron on time" and "detector on time."

If the constants for the Breit-Wigner formula are known, a calculated value for the transmission, T_c, of the sample for neutrons of energy E can be obtained from the equation

$$T_c = e^{-n'\sigma(E)}$$

Here n' is the number of atoms per cm^2 of the absorbing material and $\sigma(E)$ is the cross section of the material at the energy E as given by the Breit-Wigner formula. This, however, is not the curve that is observed experimentally, because the apparatus does not have infinitely sharp resolution. To match the experimental curve, it is necessary to include the effect of the resolution width of the apparatus.

The actual observed transmission curve is given by

$$T = \int_{-a}^{+a} \phi(u) T_c(E+u)\,du,$$

where ϕ (u) is the smearing function representing the resolution width of the aparatus on the energy basis and the a is the half-width of the resolution function.

The observed transmission at a particular energy in the vicinity of a resonance can be quite different from the calculated transmission of the sample at this point. Therefore, the observed transmission value at the minimum of the transmission dip is not a reliable measure of the amount of the resonance absorber. This problem is similar to that encountered in optical spectroscopy, where the resolution width of the spectrometer is much wider than the absorption band.

Area of the resonance dip. The difficulty noted can be circumvented by considering the integrated effect of the level over the energy range where it is effective. Let us define a quantity A which is given by the expression

$$A = \int_{E_1}^{E_2} (1-T)\,dE$$

where E_1 is less than E_0 and E_2 is greater than E_0. Quantity A represents the area between the observed resonance transmission curve and unity transmission and is proportional to what we shall call the "strength of the resonance level." The quantity A cannot be determined analytically for all cases encountered experimentally, but must be determined by numerical integration. However, when the energy of the resonance, E_0, is much greater than the width of the level, Γ, A can be evaluated exactly for the case of a very thick sample ($n\sigma_0 >> 1$) and for the case of a thin sample ($n\sigma_0 << 1$). These results are

$$A_{\text{thick}} = \sqrt{\pi n'\sigma_0\Gamma^2} \text{ or } n' = \frac{A^2_{\text{thick}}}{\pi\sigma_0\Gamma^2}$$

and

$$A_{\text{thin}} = \frac{\pi}{2} n'\sigma_0\Gamma \text{ or } n' = \frac{2A_{\text{thin}}}{\pi\sigma_0\Gamma}$$

A more complete treatment of this method is given in an article by Havens and Taylor (*2*), in which corrections to the thick and thin sample approximation have been calculated for all values of $n\sigma_0$. The procedure for obtaining more detail about the samples by fitting calculated curves to experimental data by numerical integration has been given by Havens and Rainwater (*23*).

EXAMPLE OF THE RESONANCE ABSORPTION METHOD

Application of the resonance absorption method to the specific case of the hafnium impurity in zirconium will illustrate the procedure for a typical analysis. In the transmission dip for the 16.3 g/cm^2 or zirconium shown in Fig. 15, the constant part of the observed transmission is $T = 0.496$. The observed transmission at each point is divided by 0.496, and the corrected transmission curve is then replotted. For the level at 70 μsec/m (1.07 ev) the area between this corrected transmission curve and unity transmission is evaluated by numerical integration and found to be $A_t = 10.4$ μsec/m.

Since the minimum in the corrected transmission curve is close to zero, the thick sample approximation is used. Substituting the known value of $\sigma_0\Gamma^2 = 38$ for this level of hafnium, and the experimental value of the area A_t into the thick sample formula, gives $n' = 8.4 \times 10^{20}$. The value of σ_0 for this level is 3,800b, so that $n'\sigma_0 = 3.2$, which shows that the thick sample approximation is not very good. The correction factor (*2*) for a value of $n'\sigma_0 = 3.2$ is about 19%, which means that $n' = 9.8 \times 10^{20}$, or 0.29 g/cm^2 hafnium. This corresponds to a 1.7% impurity of hafnium in the zirconium, with an estimated error of ±10% in the hafnium content. This is in reasonable agreement with the spectrographic analysis of 1.9% Hf. When a more precise numerical analysis of these data is made, the results can be obtained with higher accuracy. Also, direct comparison with standards of known hafnium content can be used to improve the accuracy of the determinations. A more complete analysis of this and other cases will be published in the near future.

To be determinable in small amounts by the method noted, the Breit-Wigner constants σ_0 and Γ should be known, and the amounts of the element in the neutron beam should be such that $n'\sigma_0$ is not smaller than about 0.2. Otherwise, the transmission at the resonance is too great for good measurements. For hafnium, using the 1.07-ev level, this means a foil containing 15.7 mg/cm^2 can be determined to about ±10%. For indium, a foil containing about 1.5 mg/cm^2 (0.002 mm thick) can be determined to within about ±10%, and calculations for gold with $\sigma_0\Gamma^2 = 612$, $\sigma_0 = 24{,}000$ barns, and $\Gamma = 0.16$ show that 2.74 mg/cm^2, or a thickness of 0.0014 mm, is determinable.

DETECTABILITY OF A RESONANCE

Actually, the minimum quantity that can be determined depends upon the energy at which the resonance occurs and the constants of the nuclear resonance, as shown by the following considerations.

Because the data taken with the neutron spectrometer are usually on the time-of-flight basis, the expression given previously for the area of the resonance dip on the energy basis should be converted to the area on a time-of-flight basis. Since $dE/E = 2dt/t$, it can be shown (*2*) that

$$\sqrt{n'\sigma_0\Gamma^2} = \frac{2\quad E_0}{\sqrt{\pi}\,t_0} A_t,$$

where A_t represents the area on time-of-flight basis.

Experimentally the criterion for a resonance level is not the area under the resonance dip but the change in transmission at exact resonance. It is difficult to give exact criteria for the strength and energy of the level for a specified transmission, because the actual observed minimum transmission depends on the resolution width of the apparatus and the actual nuclear constants of the level. However, we can examine the conditions at the two limiting cases of the resolution width of the apparatus: (1) when the level is completely resolved, and (2) when the resolution width is much wider than the resonance. For these cases the minimum observable number of atoms/cm^2 can be estimated.

In the case of Cd, the level has been completely resolved with $E_0 = 0.180$ ev, $\Gamma = 0.115$ ev, and $\sigma_0 = 7{,}200$ barns. The minimum transmission will be at the resonance energy E_0 when $T = e^{-n'\sigma_0}$. The maximum ratio of the constant transmission to the resonant transmission that can be observed is about 0.9, or $n'\sigma_0 \cong 0.1$, which gives $n' = 1.39 \times 10^{19}$ or 2.6 mg/cm^2.

For Mn, where $E_0 = 335$ ev and $\Gamma \cong 13$ ev, with $\sigma_0\Gamma^2 = 1.4 \times 10^6$, the difference in time-of-flight between the resonant neutron and a neutron of energy $E_0 \pm \Gamma$ corresponds to about 0.08 μsec/m. Since the best resolution width so far obtainable is about 0.9 μsec/m, the observed width of the resonant dip on the time-of-flight basis will be almost completely due to the resolution width of the apparatus. In the case of Mn, if the production interval τ equals the detection interval, the observed transmission dip will be triangular in shape and have a base equal to twice the interval τ. Using the maximum ratio of the constant transmission to the resonant transmission as 0.9,

$$n' = 1.3 \times 10^{19}, \text{ or } 1.4 \text{ mg/cm}^2.$$

For Mn, $\sigma_0 \cong 7{,}800$ barns; therefore $n'\sigma_0 = 0.1$, which means the thin sample approximation is the proper approximation to use.

It should be emphasized that even though the strength of the Mn level is more than 2,000 times the strength of the Cd level, the same number of atoms of Mn as of Cd must be present to obtain an observable effect. In the higher energy region, it is necessary to use a relatively thicker sample for determination of a resonance dip.

ANALYSIS BY SIMPLE TRANSMISSION MEASUREMENTS

In certain simple systems where the nature of the sample is known, it is possible to make an analysis by single transmission experiments. To reduce interferences, it may be advantageous to measure the transmission at a particular velocity, using a spectrometer or a resonance detector. In other cases, the transmission of an energy band of neutrons or of a beam of thermal neutrons may give the information desired.

To make an analysis by one of the above transmission measurements, the intensity of the beam is measured, first, without the sample in the beam (I_0) and then with the sample in the beam (I). This gives the transmission $T = I/I_0$. As shown above, the number of atoms in the beam is related to the transmission by the equation

$$-\ln T = \Sigma_i n'_i \sigma_i,$$

where n'_i is the number of atoms of *i*th kind per cm^2 and σ_i is the cross section of the *i*th atom in cm^2.

If the cross section and the amount of one element are such that they cause practically all the decrease in the intensity of the neutron beam, then the effect of the other elements can be neglected, and the number of atoms of the elements per cm^2 is given by

$$n' = -\frac{\ln T}{\sigma}$$

or

$$\mu = \frac{(-\ln T)M}{N\sigma},$$

where μ is the grams/cm^2 of the element, M is its atomic weight, and N is Avogadro's number. The percentage of the element is then given by

$$\% \text{ of element} = \mu/G \times 100,$$

where G is the total grams/cm^2 of the element and the matrix in which it occurs.

Binary mixtures in which one element has a greater cross section than the other can be analyzed if the cross sections of the two elements are known. In this case, it is necessary to know both the thickness and the density of the sample to give the total grams of material per cm^2. For such a mixture

$$-\ln T = (n'_A\sigma_A + n'_B\sigma_B) = \frac{\mu_A\overline{N}}{M_A}\sigma_A + \frac{\mu_B\overline{N}}{M_B}\sigma_B$$

μ_A and μ_B are the grams/cm^2 of substances A and B; M_A and M_B are their respective atomic or molecular weights. Since the total grams/cm^2 of the sample is $G = \mu_A + \mu_B$, then $\mu_B = G - \mu_A$. Substitution in the equation above gives

$$-\ln T = \mu_A \frac{\overline{N}}{M_A}\sigma_A + (G - \mu_A)\frac{\overline{N}}{M_B}\sigma_B,$$
$$= \mu_A K_A (G - \mu_A) K_B,$$

where $K_A = N\sigma_A/M_A$ and $K_B = N\sigma_B/M_B$. Since T, G, and the constants K_A and K_B are known, μ_A may be calculated. Then

$$\% \text{ of } A = \frac{\mu_A}{G} \times 100$$

Instead of direct calculations using the known cross section of the elements, it may be advantageous in many cases to prepare standards containing known concentrations of the element in a matrix similar to that of the unknown. Then, from a plot of $-\ln T$ vs. μ, the value of μ for the unknown can be read. Alternatively, if the sample is the appropriate type, the addition technique can be used. When the transmission of the unknown sample has been obtained, the measurement can be repeated after adding more known amounts of the element being determined. Using the linear relationship of $-\ln T$ vs. μ, one can calculate the amount of the element initially present.

Examples of cases in which analysis by simple transmission measurement may be applicable are cadmium in alloys with lead, bismuth, and tin; thickness of electroplated films of such elements as gold, silver, rhodium, cadmium, manganese, etc., on a base material of low cross section; hafnium in zirconium, indium in tin, tantalum in columbium; certain rare earths; hydrogen combined with, or dissolved in, metals; hydrogen in organic compounds; water in nonhydrogen-containing materials; etc. An interesting application of the above methods was the determination of hydrogen in fluorocarbons (*24*). It was possible to show, for example, that a sample submitted for analysis had 9.9 fluorine atoms/1,000 replaced by hydrogen.

In general, any element that has a high cross section can be determined if it is in a matrix or on a base material that has a relatively lower cross section. A partial list of elements with high cross sections in the thermal region is given in Table 5. The values are total cross sections (absorption plus scattering) for a neutron energy of 0.025 ev. They have been estimated from data reported in the literature, primarily from compilations such as the ones by Way *et al.* (*25*).

ABSORPTION OF THERMAL NEUTRONS

If an element that absorbs neutrons is placed in a region where there is a flux of neutrons, the reduction in the flux is a measure of the quantity of the neutron-absorbing elements. An example of the procedure for use with a radium-beryllium source is the determination of boron in a sample of boron carbide (*26*). The sample is ground until the particle size is below 325 mesh. This material is suspended in vigorously stirred water that surrounds a neutron detector. The assembly is placed in a block of paraffin in which the neutron source is embedded. After measuring the neutron intensity with the detector, the sample is removed, and the quantity of boron required to reduce the flux to the same value is determined by addition of a boron compound of known purity. By this method it was possible to determine that a 3- to 4-g sample of boron carbide contained 59.5% boron. Similar absorption methods can be used in the chain-reacting pile.

TABLE 5

TOTAL CROSS SECTIONS FOR THERMAL (.025 EV) NEUTRONS

Element	Cross section (barns)	Element	Cross section (barns)	Element	Cross section (barns)	Element	Cross section (barns)
A	1.4	Ga	19	Ni	22	Tl	13
Ag	66	Gd	42,000	O	4.2	Tm	114
Al	1.6	Ge	6.0	Os	29	V	12
As	9	H	(60–30)	P	4.5	W	23
Au	104	He	1.5	Pb	8.5	Xe	37
B	718	Hf	175	Pd	11.2	Y	4
Ba	9.3	Hg	400	Pr	16	Yb	50
Be	6.9	Ho	52	Pt	16.6	Zn	4.5
Bi	9.1	I	10.3	Rb	12.6	Zr	8
Br	11.5	In	194	Re	98		
C	4.8	Ir	450	Rh	155		
Ca	4.4	K	8.2	Ru	9		
Cd	2470	Kr	24	S	1.6		
Ce	6	La	18	Sb	8.3		
Cl	55	Li	70	Sc	22		
Co	41	Lu	115	Se	21		
Cr	7.3	Mg	3.0	Si	2.2		
Cs	50	Mn	15.3	Sm	8900		
Cu	11	Mo	9.6	Sn	4.6		
Dy	1150	N	12.7	Sr	11		
Er	200	Na	4.5	Ta	25		
Eu	4800	Nb	6.4	Th	55		
F	4	Nd	72	Te	10		
Fe	13.5	Ne	2.8	Ti	20		

The pile reactivity method also depends upon the absorption of neutrons by the element to be determined. It is based on the fact that the introduction of a neutron-absorbing substance in a pile decreases the reactivity of the pile (*27*). To keep the power level constant, the control rods must be withdrawn a certain distance. By proper calibration with standards, a determination can be made of the weight of absorber in the sample, provided unknown interfering substances are not present.

The *pile oscillator* may also be applied to analysis in special situations (*28*), although its primary use is to measure absorption cross sections. Here, a sample containing a substance of high absorption cross section is passed back and forth close to a neutron counter suitably placed in the graphite of the pile.

The oscillation of the sample produces uniform fluctuations in the ion current of the detector in response to local depressions in the neutron flux as the sample passes the detector. Alternatively, the sample is passed in and out of the pile to produce a fluctuation in the power of the pile. Suitable amplifier and integrator circuits measure the magnitude of the effect.

A comparison of the effect for the sample with the appropriate standards would enable the estimation of the percentage of the absorber in the sample.

NEUTRON ACTIVATION

The radioactivation of foils of suitable elements is frequently used to measure neutron flux, as explained in the previous discussion. Radioactivation is also a powerful tool for the determination of certain elements. It is particularly valuable for the determination of elements in very small concentrations. Inasmuch as this method has been recently reviewed (*3*), only a brief discussion will be given here.

The sample to be analyzed is placed in a flux f of neutrons for a time sufficient to produce a measurable activity as a result of absorption of neutrons by the element sought. The rate of growth of radioactive atoms N^* is given by the difference between the rate of formation of active atoms and their rate of decay:

$$dN^*/dt = f\sigma_{ac}N - \lambda N^*.$$

Integration for the time of irradiation gives the equation

$$N^* = \frac{f\sigma_{ac}N}{\lambda}(1 - e^{-\lambda t_1}),$$

from which the activity is

$$A_{t_1} = N^*\lambda = f\sigma_{ac}N(1 - e^{-\lambda t_1}) = f\sigma_{ac}N(1 - e^{-0.693 t_1/T^{1/2}}),$$

where f is neutron flux in neutrons/sq cm/sec; σ_{ac} is the cross section for the absorption of neutrons in sq cm/atom for the natural element; N is the number of target atoms; and λ is the decay constant for the radioactive isotope, which may be expressed in terms of its half-life $T^{1/2}$ by $\lambda = 0.693\ T^{1/2}$. A_t is the activity in disintegrations per second at the time t_1, when the neutron irradiation is stopped. These equations show that irradiation for a period of time equal to several half-lives gives practically the maximum activity obtainable ($f\sigma_{ac}N$), and that irradiation for a period of time equal to a half-life gives one half the maximum value.

If the activity is measured at a time t_2 after the irradiation was stopped, the disintegrations per second A_{t_2} will be given by:

$$A_{t_2} = A_{t_1}e^{-\lambda t_2}$$

or, combining with the above equations,

$$A_{t_2} = f\sigma_{ac}N(1 - e^{-0.693 t_1/T^{1/2}}) \times (e^{-0.693 t_2/T^{1/2}})$$

The number of atoms N of an element in a sample of weight g is

$$N = 6.02 \times 10^{23} \times g/M,$$

where M is the atomic weight. Substituting for N and then solving for g, the weight of the element in the sample is:

$$g = \frac{A_{t_2}M(e^{-0.693 t_2/T^{1/2}})}{6.02 \times 10^{23} f\sigma_{ac}(1 - e^{-0.693 t_1/T^{1/2}})}.$$

To calculate the weight of the element in the sample, it is necessary to know the neutron flux, the cross section for activation, and the half-life. In addition, the number of disintegrations per second must be determined rather precisely. This is not easy to do, because the actual count observed with the Geiger-Muller counter, for example, must be corrected for counter efficiency for the radiations; geometry (fraction of the solid angle effective in the counting); absorption of radiations by the walls, air, and the sample itself; forward scattering from the sample or surroundings; and backscattering from the sample mount, etc. All these factors tend to affect the net counting yield, which, for most cases, falls between 5 and 35%.

As a result, it is difficult to determine precisely the weight of the element from counting on a single unknown sample. Orders of magnitude or limiting concentrations are, however, frequently of interest. For example, a measured count of 2,200/minute for manganese ($\sigma_{ac} = 12$) taken directly after a saturation irradiation in a flux of 10^9 neutrons per second would, assuming a counting yield of 25%, indicate the presence of approximately 1 μg of Mn in the sample.

More precise determinations can be made by comparing the unknown sample with standards of similar composition. The unknown and standard are irradiated, and then counted, under as nearly identical conditions as possible. The weight of the element χ in the unknown is then given by:

$$\frac{\text{weight of } \chi \text{ in unknown}}{\text{weight of } \chi \text{ in standard}} = \frac{\text{activity from } \chi \text{ in unknown}}{\text{activity from } \chi \text{ in standard}}.$$

If chemical operations are necessary to remove bulk constituents or interfering radioactive elements, then both standard and unknown are treated in the same way. The element of interest is finally isolated, and its activity is determined and compared with the standard. To be certain of the radiochemical purity of the isolated element, it is advisable to determine its half-life and its aluminum or lead absorption curve. The resolution of the decay curve and the characterization of the radiations may also give valuable qualitative information about the presence of other elements. In fact, it may be desirable to run such a preliminary qualitative analysis on a sample before making the chemical separations.

When the element to be determined is present in trace amounts, a small known amount of the naturally occurring element is added after irradiation. This serves as a "carrier" to aid in the separation and isolation of the element. It also serves as a means of determining the "chemical yield" of the processes. The observed counting rates for the standard and unknown samples can then be corrected for chemical losses. In addition, corrections for self-absorption may be needed if the weights of the compounds counted are appreciably different for standard and unknown.

The principal source of uncertainty in such determination by the comparison method is the uncertainty in the counting rate. It is estimated that trace constituents can be determined with an accuracy of ±10%, which, for trace and impurity analysis, is frequently sufficient.

The sensitivity of the method is illustrated by the following. If an element such as manganese with an absorption cross section of about 10 barns is placed in a neutron flux of about 10^{12} neutrons/cm^2, about 10^{-10} g will produce a counting rate of about 100 counts per minute, assuming a 25% counting yield. This phenomenal sensitivity is only obtained with very high neutron fluxes because, with a 1-g radium-beryllium source where the usable flux for activation is about 10^5 neutrons/cm^2/sec, it would take about 1 mg of manganese to give the same counting rate. Consequently, for low neutron fluxes, the method is not too sensitive. These low intensity sources, however, may find special applications in alloy or ore analysis where high sensitivity is not required. With a chain-reacting pile where high neutron fluxes are available, 50–75 of the stable elements have properties that are more or less suitable for determination by the activation method.

For practical application the element should have a sufficiently high activation cross section (*2, 25*), and the radioisotope produced should have a half-life not less than 30 seconds for longer than a few days. In cases where the neutron properties of the individual isotopes of the elements are known and have suitable properties, the isotopic ratio in samples can be determined in a similar way by the activation method.

The activation method is not limited to the use of neutrons. Charged particles from cyclotrons and electrostatic generators have also been used successfully (*29*).

References

1. Bethe, H. A., and Backer, R. F. *Rev. Modern Phys.,* **8**, 83 (1936) ; *ibid.,* **9**, 69 (1937) ; Livingston, M. S., and Bethe, H. A. *Ibid.,* 245 ; Rainwater, L. J. *Trans. N. Y. Acad. Sci.,* II (II), 68 (1949).
2. Taylor, T. I., and Havens, Jr., W. W. *Nucleonics,* **5**, (6), 4 (1949) ; Havens, Jr., W. W., and Taylor, T. I. *Ibid.,* **6**, (2), **66** (1950) ; *ibid.,* (4), 54 (1950).
3. Boyd, G. E. *Anal. Chemi.,* **21**, 335 (1949).
4. Paneth, F. A. *Radioelements as Indicators.* New York : McGraw-Hill (1928) ; Henriques, F. C., and Margnetti, C. *Ind. Eng. Chem. Anal. Ed.,* **18**, 476 (1946).
5. Wollan, E. O., and Shull, C. G. *Science,* **108**, 69 (1948) ; *ibid., Nucleonics,* **3**, (1), 8 ; (**2**), 17 (1948) ; Hughes, D. J. *Ibid.,* **6**, (2), 5 ; (5), 38 ; (6), 50 (1950).
6. Rainwater, L., *et al., Phys. Rev.,* **71**, 65 (1947) ; Hanson, A. O., Taschek, R. F., and Williams, J. H. *Rev. Mod. Phys.,* **21**, 635 (1949) ; Tyren, H. *Svedberg Memorial Volume,* Uppsala : Almquist & Wiksells, 224 (1945) ; Seidl, F. G., and Harris, S. P. *Rev. Sci. Instruments,* **18**, 897 (1947) ; McCallum, K. J. *Nucleonics,* **5**, (1), 11 (1949) ; Russel, B., *et al., Phys. Rev.,* **73**, 545 (1948).
7. Dunning, J. R., *et al., Phys. Rev.,* **48**, 704 (1935).
8. Fermi, E., Marshall, J., and Marshall, L. *Ibid.,* **72**, 193 (1947).
9. Selove, W. A. *Ibid.,* **76**, 187 (1949).
10. Johnson, G. W., Palevsky, H., and Hughes, D. J. *Ibid.,* **82**, 345 (1951).
11. Zinn, W. H. *Ibid.,* **70**, 102 A (1946) ; **71**, 752 (1947) ; Borst, L. B., *et al. Ibid.,* **70**, 108 A, 557 (1946).
12. Rainwater, L. J., and Havens, Jr., W. W. *Ibid.,* 136.
13. Rainwater, L. J., *et al. Ibid.,* **71**, 65 (1947).
14. Goldsmith, H. H., and Rasetti, F. *Ibid.,* **50**, 328 (1936) ; Tittle, C. W. *Nucleonics,* **8**, (6), 5 ; **9**, (1), 60 (1951).
15. Marshall, J. AEC Declassified Document MDDC-78.
16. Hanstein, H. B. *Phys. Rev.,* **59**, 489 (1941).
17. Bohr, N. *Nature,* **137**, 344, 352 (1936).
18. Fermi, E., and Marshall, L. *Phys. Rev.,* **72**, 408 (1947).
19. Ruderman, I. W., *et al. Ibid.,* **75**, 895 (1949) ; Ruderman, I. W., *Ibid.,* **76**, 1572 (1949) ; Halpen, O., and Johnson, M. H. *Ibid.,* **51**, 992 (1937) ; **52**, 52 (1937).
20. Goldhaber, M. *Slow Neutron Reactions.* Brookhaven Chemistry Conference No. 3 (July 1949) ; Abst., Washington meeting, Am. Phys. Soc. (April 1949) ; Yalow, A. A. and Goldhaber, M. *Phys. Rev.,* **68**, 99 (1945).
21. Melkonian, E. *Ibid.,* **76**, 1744, 1750 (1949).
22. Adair, R. K. *Rev. Mod. Phys.,* **22**, 249 (1950).
23. Havens, Jr., W. W., and Rainwater, L. J. *Phys. Rev.,* **70**, 154 (1946).
24. Burger, L. L., and Rainwater, L. J. AEC Declassified Document, AECD-2138 (1948).
25. Way, K., *et al. Nuclear Data.* Cir. Natl. Bur. Stand. No. 499 (1950).
26. Walker, R. AEC Declassified Document, MDDC-362 (1946).
27. Anderson, H. L., *et al. Phys. Rev.,* **72**, 16 (1947).
28. Hoover, J., *et al. Ibid.,* **74**, 864 (1948).
29. Searorg, G. T., and Livingood, J. J. *J. Am. Chem. Soc.,* **60**, 1784 (1938) ; King, D. T. P., and Henderson, W. J. *Phys. Rev.,* **56**, 1169 (1939) ; Sagane, R., Equchi, M., and Shigeta, J. *Proc. Phys. Math. Soc. (Japan),* **16**, 383 (1942) ; *Chem. Abs.,* **41**, 7303 i (1947) ; Ardenne, M., and Bernhard, F. *Z. physik.,* **122**, 740 (1944).

* * *

The **Wayne University** biennial "Frontiers in Chemistry" lecture series began on Sept. 24 with a lecture by John G. Ferris, of the U. S. Geological Survey. Ng. Ph. Buu-Hof, of the Institut du Radium, Paris, spoke on Oct. 1, and on succeeding Monday evenings the following speakers will be presented: Harvey Diehl, C. S. Marvel, Robert S. Mulliken, G. B. B. M. Sutherland, and H. J. Emeléus (Cambridge University). Additional information may be obtained through George H. Coleman, Kresge-Hooker Scientific Library. Dr. Coleman is currently serving as head of the Chemistry Department during the tenure of J. Russell Bright as associate director of the newly organized Division of Contract Services at Wayne. John R. Richards, executive assistant to the president, has been serving as director.

James E. Lofstrom has been appointed special professor of radiology and chairman of the division in the Wayne University College of Medicine. The appointment was made jointly with Receiving Hospital, where Dr. Lofstrom has been named head radiologist. Funds for the university's contribution to his salary are available through a special grant from the National Fund for Medical Education. Dr. Lofstrom has been a member of the Wayne faculty since 1935.

Joseph M. Looney, chief of laboratories at the regional office of the Veterans Administration, Boston, has been appointed research professor of biochemistry at the Boston University School of Medicine. He is also consultant in endocrinology at St. Elizabeth's Hospital.

Frederick Morgan has been appointed controller of atomic energy in Britain. General Morgan succeeds Viscount Portal of Hungerford, chief of the British air staff during the war, who resigned.